JOURNAL OF CATALYSIS 67, 129–144 (1981)

Atom Superposition and Electron Delocalization (ASED) Theory for Catalysis. Dissociative Properties of Acetylene on Fe and Ni(100) with Coadsorbed O, S, Se and Implications for Te[1]

ALFRED B. ANDERSON[2]

Chemistry Department, Yale University, New Haven, Connecticut 06520, and Department of Chemistry, University of California, Santa Barbara, California 93106

Received October 10, 1979; revised October 19, 1980

Using an atom superposition and electron delocalization (ASED) theory, acetylene is found to bond to the fourfold site on Ni(100) more strongly and with greater C–C bond lengthening distortion than on Ni(111). Half-monolayer $c(2 \times 2)$ O, S, Se, and Te coverages poison the surface toward acetylene chemisorption. Quarter-monolayer (2×2) O and S allow weakened adsorption. A specific destabilization of an acetylene π orbital when bridging two O atoms activates C–C bond scission barrier reduction. This is of catalytic significance. Increasing or decreasing the surface Ni charge, as occurs when bonding to more electronegative or electropositive atoms or on an electrode in a dielectric medium, also serves to weaken the barrier. The bonding of S and Se to Fe(100) is treated. The fourfold site is preferred because a high-lying orbital loses its unpaired electron in this site. On quarter-monolayer covered Fe(100), acetylene C–C bond scission is accelerated in chalcogen bridging sites by the same wedging effect even though the chemisorption energy is weakened. Chemisorption occurs only on the half-monolayer $c(2 \times 2)$ O-covered surface if a high-lying orbital loses its unpaired electron. This possibility is discussed. The relationship of the theory and photoemission spectra is discussed.

I. INTRODUCTION

Theory can play a role in the development of our understanding of structures and reactions of atomic and molecular surface species. There is an impetus to understand the details of surface catalyzed reactions such as the hydrogenolysis of coal (*1*) and the hydrogenation of unsaturated hydrocarbons (*2*). Recent theoretical (*3*) and experimental (*4*) studies show pure iron to be too reactive toward acetylene or ethylene to allow hydrogenation and desorption of alkanes. Since coal is hydrogenated over iron, oxygen, sulfur, or other impurities in coal or carbon itself must be altering the properties of the iron surface. Contrasted to this, nickel, a good hydrogenation catalyst, is rapidly poisoned by sulfur. Theoretical and experimental studies attempt to explain the different properties of the iron and nickel surfaces.

The strong interaction of pure iron with unsaturated hydrocarbons discussed in (*3, 4*) is a result of strong back-bonding into the antibonding π^* orbitals. Theoretical (*5*) and experimental (*6*) studies both show weaker interactions between acetylene and the Ni(111) surface, such that acetylene does not undergo C–C bond scission at room temperature as it does on Fe(100). This is attributed in Ref. (*5*) to the more diffuse *d* orbitals in iron.

Structures and reactive properties of acetylene and other C_2 hydrocarbon molecules on Pt(111) are of current interest (*7–10*). Despite difficulties inherent in surface spectroscopies, ultraviolet photoemission (UPS) (*7*), dynamic low-energy electron diffraction (LEED) (*8*), and electron energy loss (EELS) (*9*) spectroscopic analyses are making substantial headway in providing structural information. Our theoretical cal-

[1] Research supported by the National Science Foundation.

[2] Present and permanent address: Chemistry Department, Case Western Reserve University, Cleveland, Ohio 44106.

0021-9517/81/010129-16$02.00/0

culations (*10*) have confirmed the recent electron energy loss vibrational analysis (*9*) which finds acetylene bound at low temperature at a triangular site with a C–C bond stretch of 0.24 Å and an HCC bend up from the surface of 60°. Calculations produce 0.30 Å and 55°, respectively. According to a dynamic LEED study (*8*), at around 400°K acetylene rearranges and picks up ambient hydrogen to become ethylidyne, CCH_3, standing up in a triangular site with Pt–C distances of 2.0 Å and a C–C bond 0.30 Å longer than that in gas-phase acetylene. Our calculations produce 2.0 and 0.35 Å, respectively.

A similar theoretical study of acetylene on Ni(111) favored a μ/π site with a C–C bond stretch of 0.17 Å and an HCC bend of 50°, though early UPS studies were interpreted in terms of a π site (*6, 7*). An EELS study led independently to the μ/π structure (*11a*) and the UPS spectra were found consistent with this (*11b*). The EELS study produced a stretch of 0.15 Å and a bend of 55°.

These results not only illuminate the usefulness of the EELS method and the ASED theory for determining surface structures, but show the richness of the structural chemistry for acetylene on simple surfaces. They demonstrate theory can have predictive as well as interpretative power. Consequently this paper deals in predictions.

Little experimental work has yet been done with acetylene chemisorbed on the surfaces studied here. Yet surfaces with oxygen, sulfur, and other chalcogen atoms are sometimes good catalysts and sometimes passive. This paper analyzes these properties with model systems.

Attention is focused on how coadsorbed chalcogen atoms affect chemisorption energies, C–C bond strength, and C–C bond scission barriers. This is accomplished in terms of the effects of ionic shifts of the metal s–d band, specific orbital interactions, and special attention is given to the structural effects of high-spin and low-spin electron coupling. Concepts of orbital size, the general weakening of interactions as shells of levels are filled, and the connection between certain structural and electronic factors are developed. Effects of charging, as on an electrode surface, are also considered. These concepts will apply to other systems yet to be examined.

It is found that at half-monolayer coverage in O, S, Se, and Te on Fe and Ni(100) acetylene will not chemisorb. An exception may be the O on Fe(100) surface where there is probably weak chemisorption if two of the unpaired electrons pair up. The significance of this possibility is discussed. For O(2 × 2) quarter-monolayer covered Fe(100) dissociative chemisorption occurs, yielding CH with a much reduced chemisorption energy. On Ni(100) this coverage of S, Se, and Te prevents chemisorption, whereas O possesses an interesting ability to activate dissociative chemisorption. The cause lies in specific orbital interactions and occurs implicity also on the Fe surfaces, for which there are no calculated barriers. This phenomenon is expected to be a general one and it says that when the structure is appropriate the chemisorbed chalcogen atoms, and, in principle, other atoms, weaken the C–C bond in acetylene by wedging the carbon atoms apart.

II. RELATIONSHIPS INVOLVING PHOTOEMISSION SPECTRA, BONDING, AND THE ASED THEORY

Over the past half dozen years photoemission spectra for unsaturated hydrocarbon molecules chemisorbed on Ni(111) and other surfaces have been interpreted in terms of adsorption energies (*6, 12*) and structures (*7, 13*). References (*7, 12*) discuss difficulties in making these interpretations. With energies a problem is spotting all the surface-adsorbate energy level shifts and with structures it is uniqueness.

There are two reasons for the above difficulties. First, orbitals relax during the ionization process, and not all orbitals relax by the same amount (*14*). Second, the total

energy of a molecule depends on more than the orbital energy. For example, in the Hartree–Fock orbital approximation one must add the nuclear repulsion energy and subtract the electron repulsion energy which is counted twice in the total orbital energy.

The ASED theory used in this paper recognizes the total energy to be well approximated as the sum of orbital energies due to atomic electron delocalization and atom–atom pairwise repulsion energies due to atom superposition. Were the atom–atom repulsion energies constant, the orbital energy in this theory or from experimental measurements, provided relaxation shifts are small enough, would provide structure and bond strength information.

There are examples where this two-body energy is nearly constant so that changes in orbital energies correspond to changes in total energies. These cases have long been treated with Mulliken–Walsh diagrams (*15*). Such analyses are applicable to molecular bends and twists and orbital population discussions where bond lengths may be taken as fixed. Clearly this is not the case for the chemisorption of acetylene on a Ni(111) surface. However, at least one Mulliken–Walsh analysis has been made of a surface catalyzed reaction, the 1,3 sigmatropic shift in propylene over transition metal surfaces, by assuming model lengths (*16*).

Studies of dozens of systems show it is possible to predict structures, electronic energy levels, and vibrational properties of cluster, solid-state, surface, and other molecular systems with the ASED theory. Calculated bond lengths are usually within 0.05 Å of experiment and rarely more than 0.15 Å in error. Force constants are rarely in error by more than 30%. Bond energies are rarely more than a factor of 2 in error. Most importantly, the theory produces trends as observed by experimental chemists. In the study to follow the absolute numbers that are predicted are semiquantitative; the relative values are the basis of chemical understanding when combined with electron orbital analyses.

III. ASED THEORY

In the ASED theory, atoms are first superimposed and a *fundamental assumption* is made: it is assumed atomic orbital ionization energies are not shifted by fields due to neighboring atoms. Within the *fundamental assumption*, the atom superposition energy is E_R given exactly as a summation of pairwise terms,

$$E_R = \sum_{a<b} Z_b[\int \rho_a(r)/|\boldsymbol{R}_b - \boldsymbol{r}|d\boldsymbol{r} + \boldsymbol{Z}_a/\boldsymbol{R}_{ab}], \quad (1)$$

where Z is a nuclear charge, ρ is an atomic electron charge density function, $\boldsymbol{R}$ is a nuclear coordinate, and $\boldsymbol{r}$ is an electron coordinate.

Following the instantaneous atom superposition which produces E_R, the electrons begin to hop about to other atomic orbital base states according to an exact time-dependent perturbation theory (*17*). The hopping amplitudes are definite numbers for each possible change of base state. This description of electron dynamics allows for excitations and exchange of other electrons when one electron hops from one base state to another, and is therefore a configuration–interaction approach within a one-electron framework. Stationary-state solutions, where all base states vary the same way in time, lead to the secular equation $|E\delta(i, j) - h(i, j)| = 0$, where h is the hopping amplitude. Linear variational theory for one electron produces a similar secular equation leading to the identity for off-diagonal matrix elements, $H(i, j) = h(i, j) - ES(i, j)$, where H is an energy Hamiltonian, E a variational one-electron orbital energy, and S an overlap integral. This identity makes possible the hopping and configuration–interaction interpretation. The *fundamental assumption* results in the working equations for the Hamiltonian ma-

trix elements

$$H(i, j) = -I_i, \quad (2)$$

$$H(i, j) = -\tfrac{1}{2}(I_i + I_j)S(i, j), \quad (3)$$

where I is a measured atomic ionization potential. A generally more accurate formula has $H(i, j)$ in Eq. (3) multiplied by 2.25 $\exp(-0.13R)$ and this is used here. The molecular orbitals obtained allow traditional bonding analysis and the total orbital energy, E_{MO}, is added to E_R, producing useful predictions of structure, force constants, and relative bond strengths for ground and excited states, as in Refs. (*3, 5, 18*). The calculated energy levels are similar in distribution to photoemission bands minus the shake-up bands. The calculated energy levels are, within an approximation, physically observable. The diatomic contributions to E_R in Eq. (1) are also physically observable, as they contain bond stretching force constants for various diatomic states within some percentage accuracy (*18*). Thus the ASED theory splits the chemical bond energy into two parts approximating physical observables. For an interpretation based on molecular charge density functions, see Ref. (*5*).

There is a possibility of having excessive charge transfer to some atoms. Such effects are accommodated by redefining the atomic base states to incorporate the ionic charge transfer perturbation. If an atom becomes negative, its valence orbitals expand in spacial extent and their ionization potentials decrease. The swelling affects E_R since the more electronegative atom swells. Electropositive atoms contract and their ionization potentials increase. Hence, hopping amplitudes and the electron delocalization energies are also affected. References (*3, 5*) demonstrate the application of these principles.

IV. CHEMISORPTION OF ACETYLENE TO Ni(111) IN TERMS OF E_R AND E_{MO}

For fixed bond lengths in a molecule, the molecular orbital energy levels and total orbital energies are properties approximately obtainable from photoemission spectra. To this must be added E_R when binding and chemisorption energies are sought. For acetylene chemisorbed on a two-layer-thick Ni_{31} slab representing Ni(111) taken from Ref. (*5*) the contribution to E_{MO} as a function of Ni s–d band position appears in Fig. 1. Large stabilizations are visible in the $s\sigma$, $s\sigma^*$, π_y, and π_z orbitals in acetylene. It is not simply π stabilization, which contributes to the chemisorption energy, as originally believed (*6*). The σ_s stabilization, already discussed in theoretical studies of chemisorbed hydrocarbons in Refs. (*3, 5*), and further considered below, has been observed recently in the photoemission spectra (*19*). Destabilization is apparent throughout the Ni valence band in Fig. 1, particularly near the Fermi energy, E_F. This is due, in part, to the antibonding counterparts of the stabilizing metal–adsorbate orbital interactions. The π_z^* orbital mixes in with an energy just above the π_y level. This is the back-bonding interaction responsible for the 0.17 Å elongation of the C–C bond and the 50° bend of HCC away from linearity (*5, 11*).

The total orbital stabilization is 24 kcal/mole. The C–C bond stretch provides 53 kcal/mole stabilization to E_R; however, the formation of C–Ni bonds adds 34 kcal/mole destabilization. The net stabili-

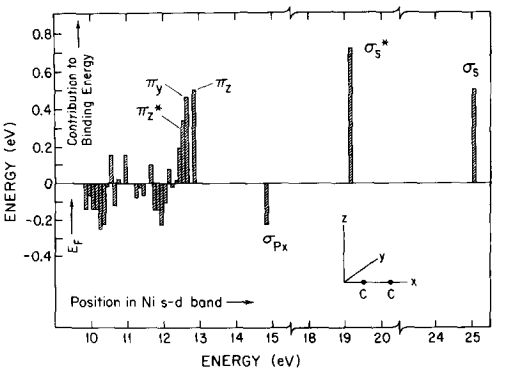

FIG. 1. Orbital contributions to the binding energy of acetylene to a Ni_{31} cluster representing the (111) surface as in Ref. (*5*).

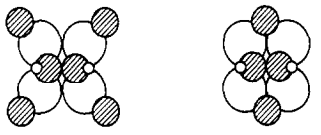

	BE	EA	BE	EA
		(kcal/mole)		
–	34	45	34	45
O	19	32	11	26
S	18	61	—	—

FIG. 2. Fe_4X_4 and Fe_4X_2 models of $p(2 \times 2)$ quarter-monolayer X = O and S coverage with adsorbed acetylene. Open circles are Ni atoms, exterior hatched circles are O and S, interior hatched circles are C, and small interior open circles are H. Drawn approximately to scale in terms of atomic radii. In the centered fourfold site the C–C bond stretches 0.24 Å, the HCC angle is 125°, and the height is 1.5 Å. For the bridging site on Ni_4X_2 the C–C bond stretches an additional 0.06 Å. Binding energies, BE, and activation energies for C–C bond scission, EA, are shown for clean and oxidized and sulfurized surface models.

zation in E_R is 19 kcal/mole. It is emphasized that this component of the stabilization will not be obtainable from photoemission spectra. The total calculated chemisorption energy is 43 kcal/mole, in good agreement with experiment as discussed in Ref. (*5*).

V. BONDING AND REACTION OF ACETYLENE ON Ni(100)

Calculations employing a square Ni_4 cluster representing Ni(100) produce results qualitatively similar to those for the diamond-shaped Ni_4 cluster representing Ni(111) (*5*). Bonding to the center (as in Fig. 2) is preferred, with the C–C axis parallel to an edge. Calculations produce a bond stretch of 0.24 Å, 0.07 Å greater than that for the (111) surface. The HCC angle is 125°, compared with 130° for the (111) surface. Reference (*11b*) also deduces a slightly weaker distortion on the basis of relative shifts of acetylene σ levels seen by photoemission spectroscopy on Ni(100) compared with Ni(111), but recognizes "a precise geometry for this more strongly distorted species cannot be deduced from (their) present analysis" in the case of Ni(111). This should also apply to Ni(100). The calculated chemisorption energy to (100) Ni_4 is 34 kcal/mole, compared to 25 kcal/mole for (111) Ni_4. On larger clusters this increases in both cases; see Fig. 3 and Ref. (*5*). The distance from the surface plane of nuclei is 1.5 Å. In a qualitative sense, the interaction is stronger because the C–C bond can stretch further on the (100) surface before C–Ni contributions to E_R become large. The stabilization in the C–C component of E_R is 63 kcal/mole. On including C–Ni contributions, the net stabilization is 23 kcal/mole. This is only 4 kcal/mole greater than the E_R stabilization on the (111) surface. Therefore E_{MO} strongly favors the (100) surface.

Throughout these calculations, parameters and orbital occupations are taken from Ref. 3. That is, I_{exp} is increased 1 eV for Ni and decreased 1 eV for C and H. This reduces charge transfer to C to a value of 0.28 electrons on (100) Ni_4. High-spin orbital occupations are employed so that each *d*-band level contains at least one electron. Thus these systems are triplets. Basic parameters are listed in Table 1.

Energy levels calculated for acetylene, (100) Ni_4, and their combination are in Fig. 4. The chemisorbed acetylene levels are close to those for (111) Ni_4 (*3*), though the increased C–C bond stretch shifts the σ levels a bit more. On a very large cluster the σ_s level will shift below the free acety-

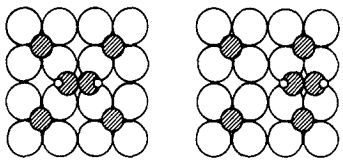

	BE	EA	BE	EA
		(kcal/mole)		
–	45	44	45	44
O	37	44	28	32

FIG. 3. Same as Fig. 2, only $Ni_{16}X_4$ models are used.

TABLE 1

Parameters Used in the Calculations before Adjustments Discussed in the Text

Atom	Principal quantum number, Slater exponent and ionization energy (eV)								
	s			*p*			*d*[b]		
O[a]	2	2.246	−28.48	2	2.227	−13.62	3	2.4	−3.0
S[a]	3	2.222	−20.2	3	1.927	−10.36	3	1.9	−4.0
Se[a]	4	2.539	−20.15	4	2.172	−9.75	4	2.2	−4.0
C[c]	2	1.658	−20.0	2	1.618	−11.26			
H[c]	1	1.2	−13.6						
Ni[c]	4	1.8	−7.635	4	1.5	−3.99	3	5.75[d]	−10.0
Fe[e]	4	1.7	−7.87	4	1.4	−3.87	3	5.35[f]	−9.0

[a] Ref. (*21*).

[b] Chalcogen *d* orbital omitted in acetylene chemisorption calculations.

[c] Ref. (*5*).

[d] Double zeta orbital. The second exponent is 2.0. Respective coefficients are 0.5683 and 0.6292.

[e] Ref. (*4b*).

[f] Double zeta orbital. The second exponent is 1.8. Respective coefficients are 0.5366 and 0.6678.

lene position, as in (*3*). This stabilization is the result of the influence of cluster size in increasing an unusual nonbonding, yet stabilizing, interaction whose orbitals are depicted in Fig. 5. Stabilization by negative overlap is unexpected. This phenomenon is

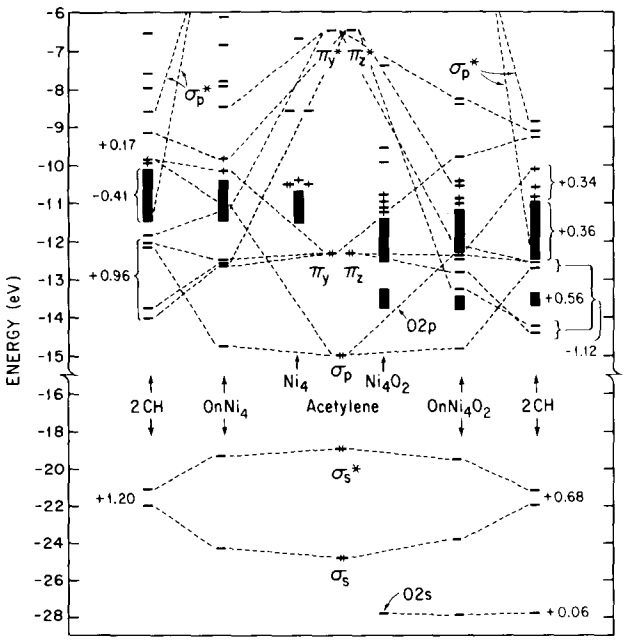

FIG. 4. Behavior of molecular orbital energy levels of acetylene and Ni_4 and Ni_4O_2 when bonding geometries as in Fig. 2 are set up. On C–C bond scission, CH levels form as shown, with the CH radicals perpendicular to the surface in Ni–Ni bridging positions, C end down.

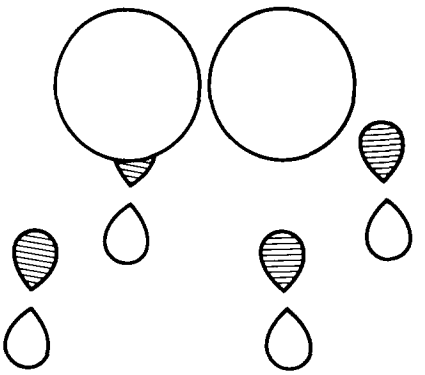

FIG. 5. Orbital behavior when the acetylene $s\sigma_g$ orbital is stabilized by negative overlap with Ni $4p$ orbitals in the Ni_4 model of the (100) surface.

important to chemisorption, particularly for saturated hydrocarbons, discussed in Ref. (*3*), and other nearly closed shell systems, such as H_2, also analyzed in Ref. (*3*). It occurs when atomic and molecular orbitals in species in proximity have large overlaps but disparate orbital energies. Its occurrence in other molecular orbital calculations has been discussed (*20*).

According to Ref. (*6*), acetylene is stable on Ni(111) up to ~470° at which point dehydrogenation occurs. Calculations produce a C–C bond scission barrier of 25–30 kcal/mole and a C–H barrier of ~45 kcal/mole (*5*). It appears that the C–C barrier is underestimated, but a temperature of 470°K is consistent with the order of magnitude of the C–H barrier. Possibly C–C bond scission is a prerequisite to C–H dissociation on Ni(111).

On the (100) surface calculations produce a C–C bond scission barrier of about 45 kcal/mole. Further, on a 2 × 4-atom Ni_8 cluster, calculations show chemisorbed associated acetylene is 10 kcal/mole more stable than two CH fragments. These fragments sit C end down 1.0 Å from in the center of four-atom squares. It seems that C–C bond scission is not a strong thermodynamic possibility. Rearrangement and hydrogenation mechanisms and energetics deserve theoretical analysis in the future.

VI. CHEMISORPTION AND DISSOCIATION OF ACETYLENE ON A CHARGED Ni(100) SURFACE

Whereas oxygen on Ni(100) increases the Ni valence ionizaton energies by approximately 2 eV (*21*), the lesser electronegativity of acetylene results in a shift of 1 eV or less. How do shifts in metal ionization energies affect acetylene chemisorption and C–C bond scission energies on Ni surfaces? Charging of the surface as an electrode in solution can also cause positive or negative shifts of 2 eV. Chemisorption or dissolution of the electropositive 1a or 2a metals should decrease metal ionization energies as O or halides increase them. These factors are considered in this section using the (100) Ni_4 model and shifting the Ni valence ionization energies.

As may be seen in comparing Table 2 with Fig. 2, if either the Ni ionization energies are increased 2 eV or the C and H ones are decreased 2 eV, the acetylene chemisorption and C–C scission energies are not far from the case of 1-eV shift for Ni, C, and H. However, for large shifts in atomic valence state ionization energies the results are nonlinear. This is the result of the off-diagonal matrix elements increasing as atomic ionization energies increase. In the cases of 2-eV Ni shift, 2-eV C, H shift, and 1-eV Ni, C, H shift, the C changes are, respectively, −0.42, −0.32, and −0.28

TABLE 2

Binding Energies, BE, and Activation Energies, EA, for Acetylene Bonding to a Ni_4 Model of the (100) Surface, as a Function of Shifts in Valence Ionization Energies, ΔI

$\Delta I_{Ni} = 0$			$\Delta I_{CH} = 0$		
ΔI_{CH}(eV)	BE[a]	EA[a]	ΔI_{Ni}	BE[a]	EA[a]
0	100	17	0	100	17
1	68	37	−1	63	37
2	50	44	−2	40	44
3	65	36	−3	36	36
4	49	24	−4	51	20

[a] kcal/mole.

electron. In all calculations in this section the geometries of Section V are employed and the transition state has CH fragments 1.45 Å above the surface, perpendicular, C end down, in bridging positions.

Figure 6 shows how energy levels for Ni_4 + acetylene change on chemisorption and dissociation as C and H ionization energies are shifted and fixed while the Ni values are increased by $\Delta I = 0$, 1, 2, 3, and 4 eV. As the Ni s–d band drops it pushes down, with bonding stabilizations, the acetylene σ_p and π energy levels. At the same time the antibonding combinations in the band become more strongly destabilizing up to a Ni shift $\Delta I = 3$. At $\Delta I = 4$ acetylene loses about 1.5 electrons to the lowered Ni s–d band and the chemisorption energy begins to increase. The acetylene σ_s^* level is relatively insensitive to the Ni band position in this range. With increasing shift the σ_s level is, on the other hand, destabilized. With $\Delta I = 4$, the Ni $4s$, $4p_x$, $4p_y$, $4p_z$, and C $2s$ coefficients for the σ_s level are 0.0209, 0.0228, 0.0249, −0.0340, and 0.5380. When the shift is 0 they are −0.0113, 0.0306, 0.0433, −0.0663, and 0.5824. Thus as the negative $4p_z$–$2s$ overlap decreases in magnitude, the level is destabilized.

The activation energy for C–C bond scission is a maximum with $\Delta I = 2$ for Ni or C and H. Since the change in E_R is the same in all cases, the lowering of the barrier on charging the Ni surface positive or negative lies in changes in electron delocalization, that is, orbital energies.

A graph of total orbital energy changes as a function of ΔI for Ni appears in Fig. 7. Groups (2) and (4), defined in Fig. 6, are large near $\Delta I = 2$. Group (3) is very negative when $\Delta I < 2$. When $\Delta I > 2$, group (1) begins to increase. It is evident that lowering the Ni s–d band pushes down the acetylene σ_p and π level which stabilizes the transition. The σ_s and σ_s^* acetylene set is stabilized at the same time mainly because the σ_s level is less stabilized by negative overlap bonding with the surface. The π_y, π_z^* antibonding set group (1) begins to rise slowly when the π levels coincide with the Ni s–d band. As the band drops further, this contribution may decrease. Finally, other contributions in the Ni band, group (3), show a large stabilization when ΔI is small, primarily from the π_y^* and σ_p^* bonding combinations with the d band. This drops to 0 when $\Delta I \sim 3$–4 eV.

It is significant that Fig. 7 is complicated and that for the C–C bond scission energy to be a maximum on the neutral surface is accidental. Further, groups (2) and (4) which would be most readily discernible in photoemission spectra, not overlapping with the s–d band, show a decrease in the

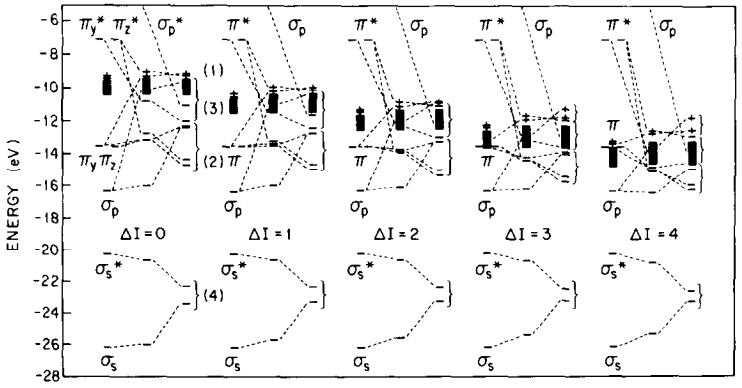

FIG. 6. Behavior of molecular orbital energy levels of acetylene and the Ni_4 model of the (100) surface before and after adsorption as a function of shifts in the Ni valence ionization potentials, ΔI. Note groups (1), (2), (3), and (4).

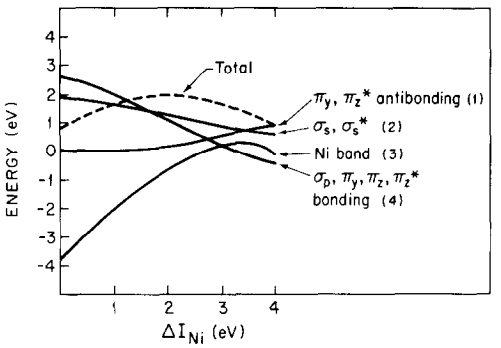

FIG. 7. Behavior of total orbital energies in groups (1)–(4), as defined in Fig. 6, as functions of ΔI, changes in Ni valence ionization potentials.

barrier as ΔI increases. Difference spectra must be used to assess the importance of groups (1) and (3).

This analysis omits hydrogenation, dehydrogenation, and rearrangement reactions. The extent to which such reactions may be catalyzed by electronic surface charging or charge transfer due to surface compound formation on single-crystal faces is a topic for future theoretical and experimental studies. At least one such study, employing approximately a monolayer of potassium on a Ni surface, exists (*22*). The experimental result is a decreased interaction between ethylene and the surface and, apparently, a lessened tendency for C–H bond scission.

VII. BONDING AND DISSOCIATION OF ACETYLENE ON O-, S-, Se- AND Te-COVERED Ni(100) SURFACES

The ASED theory of $c(2 \times 2)$ half-monolayer covered O (*21*), S, Se, and Te (*23*) on various-sized cluster models of Ni(100) has already been presented. The predictions of fourfold binding sites and heights above the surfaces are in close agreement with dynamic LEED estimates (*24*). Others recently obtained similar agreement with experiment by using a parameterized valence bond calculational procedure for 0 and S bonded to the same Ni_4 models (*25*), but results for the larger models used in Ref. (*23*) were not reported. The theoretical studies in Refs. (*21, 23*) also provide interpretations for assignments of photoemission spectra for O (*26*), S (*27*), Se (*27*), and Te (*28*), showing the $Ni^{\delta+}$ shifted *d* band for the oxide and the apparent importance of chalcogen atom final-state multiplet splittings in the *p* bands. The predicted relative vibrational force constants and chemisorption energies have yet to be measured.

In this section parameters and geometries are the same as those in Refs. (*21, 23*). For the surface oxides $\Delta I = +2$ eV for Ni and -1 eV for O. The O Slater exponents are decreased 0.2 due to ionicity. Basic parameters are listed in Table 1. For the sulfides and selenides no parameter adjustments are necessary. Neither would any be necessary for the telluride surfaces, which are not actually treated since their properties would be direct extrapolations of the weakly interacting sulfides and selenides. On the $p(2 \times 2)$ quarter-monolayer Ni_4O_4 and $Ni_{16}O_4$ models in Figs. 2 and 3, the acetylene carbon charges are 0.08 and -0.04 electron. On Ni_4S_4 the carbon charges are -0.33, close to -0.28 with S absent. In the S and Se calculations ΔI for C and H is 1 eV and acetylene is taken to cause a ΔI of -1 eV in Ni.

With $c(2 \times 2)$ half-monolayer coverage of chalcogen atoms on Ni(100), acetylene will not chemisorb. At $p(2 \times 2)$ quarter-monolayer coverage in O and S, acetylene will stick to the fourfold sites in Fig. 2. In twofold sites chemisorption occurs only for the oxidized surface. On the fourfold site, the chemisorption energy is doubled in going from Ni_4O_4 to $Ni_{16}O_4$ in Fig. 3. In the twofold site it is more than doubled. On the fourfold site on $Ni_{16}O_4$ the C–C bond scission energy is the same as on the Ni_{16} cluster, but on the bridging site it is 12 kcal/mole less. On Ni_4O_2 the activation in the twofold site is less, but present.

On Ni_4O_2 the C–C bond stretch increases 0.06 to 0.30 Å while the HCC angle is unchanged at 55°, and the height remains 1.5 Å. The tendency to dissociate more

easily in the bridging position is shown in this stretch.

The weakening of the chemisorption bond by oxygen seen in Figs. 2 and 3 is no doubt a result of antibonding interactions due to oxygen. Distances are large enough between C and O for interactions through the metal atoms to be important. The 19 and 11 kcal/mole chemisorption energies for Ni_4O_4 and Ni_4O_2 are much less than either $\Delta I = 3$ value in Table 2. For $\Delta I = 3$ the barrier to C–C bond scission is 36 kcal/mole on Ni_4O_2. Consequently, it may be said that oxygen plays a greater role in changing the chemisorption and reaction of acetylene than merely shifting the Ni s–d band by an additional 1 eV.

Figure 4 shows how, while the Ni band is lowered by another electron volt by oxygen, the stabilization of the π_y, π_z, and π_z^* orbital energy levels is much less than in Fig. 6 for $\Delta I = 3$ eV. This is because the 0.2p band pushes them up, particularly the π_y level. The destabilization of a band of levels by a nearby filled band is a common occurrence. However, when acetylene dissociates into two CH fragments, the O 2p band provides important assistance. The π_y orbital is especially destabilized by O as seen in examining the orbital overlaps in Fig. 8, but it is not more destabilized in the transition state, as it is when O is absent.

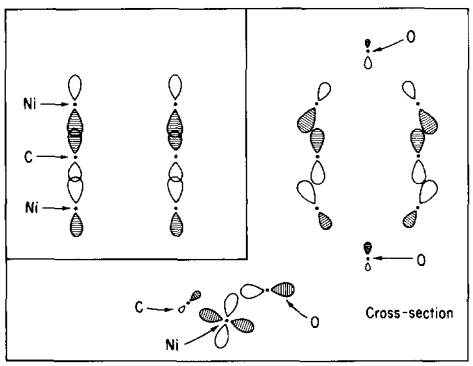

FIG. 8. Interactions of adsorbed CH fragment π_y orbital with Ni_4 and Ni_4O_2. By steering the Ni d orbitals, O weakens the Ni–C overlap and thereby destabilizes acetylene prior to C–C bond scission.

Consequently, as shown in Fig. 4, this interaction decreases the barrier by 7 kcal/mole while in the absence of O it increases the barrier by 20 kcal/mole. Oxygen also reduces the σ_p shift from 120 to 98 kcal/mole, but this also occurs on going from $\Delta I = 2$ eV to $\Delta I = 3$ eV in Fig. 6, so it is a charge effect. Without O, the net destabilization due to σ_p, π_y, π_z, and π_z^* orbitals is 22 kcal/mole. With O there is a 26 kcal/mole stabilization. The net stabilization of the transition state, 48 kcal/mole, is close to the 49 kcal/mole from the previous two effects. The unpaired electrons contribute 4 kcal/mole without O and 8 kcal/mole with it, and the Ni s–d band, 0 and 8 kcal/mole, respectively. The presence of O decreases the antibonding stabilization of the C–C σ_s orbital. The O 2_p band is destabilized by 13 kcal/mole in the transition state. Finally, the O 2_s levels contribute 1 kcal/mole. E_R increases 6 kcal/mole on the oxidized surface because the 0.06-Å additional C–C bond stretch reduces E_R for chemisorbed acetylene. Without oxygen, the increase is only 1 kcal/mole. The net result, including corrections for roundoff errors in these numbers, is that the barrier to C–C bond scission is reduced 19 kcal/mole by oxygen on Ni_4O_2.

This complicated analysis suggests elements of a simpler picture. The oxygen atoms orient a Ni d band orbital so that it does not stabilize the acetylene π_y orbital as much as if just the ionic s–d band shift were operative. This weakens the chemisorption energy, so that the transition state is less destabilized. In addition, the ionic s–d band shift drives down the $p\sigma$ orbital in the transition state, whether or not oxygen is present. These effects, plus several smaller ones, lower the barrier by 19 kcal/mole on Ni_4O_2 and by 12 kcal/mole for the bridging site on $Ni_{16}O_4$. In the fourfold site it is lowered by 13 kcal/mole on Ni_4O_4 and by nothing at all on $Ni_{16}O_4$. The $Ni_{16}O_4$ results should better represent the surface.

Recent photoemission studies (29) show

that when acetylene is chemisorbed on a Ni(111) surface already covered by (2 × 2) oxygen, a new species forms which appears to be CH radicals. Calculations with smaller cluster models show O reduces the C–C bond scission barriers. Although a detailed analysis is not presented here, it may be inferred that the same orbital interactions are operative here as for the oxidized (100) surface.

It may be seen in Fig. 3 that the centered site on $Ni_{16}O_4$ is 9 kcal/mole more stable than the bridging site. An analysis of the orbital energy levels for the two systems appears in Fig. 9. The π_y level contributes 15 kcal/mole to the relative stability of the centered site, more than any other group of levels. Figure 10 shows the antibonding O—C interaction which decreases the stability of the bridged site. This orbital steering effect, caused by the O atoms is a "through-bond" (*30*) interaction. It reduces the C atomic electron population from 0.42 to 0.18 electron in the π_y orbital. This, however, is not the exclusive orbital with acetylene π_y character; it is the major orbital. As always, more minor hybridization throughout the metal *d* band occurs for

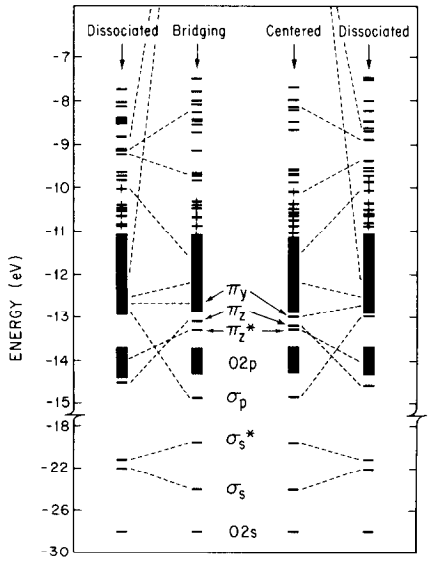

FIG. 9. Molecular orbital energy levels for acetylene and CH fragments as in Fig. 3.

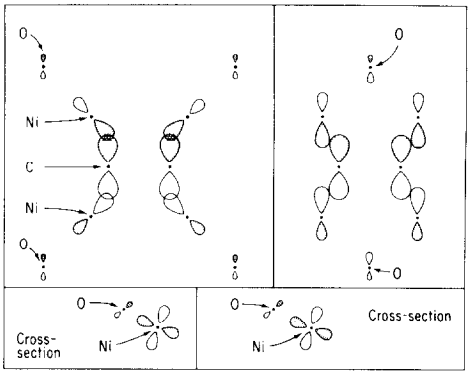

FIG. 10. The extra stability of the π_y orbital seen in Fig. 9 for the centered site is a result of better overlap with Ni *d* orbitals as depicted here.

this and all other acetylene orbitals. Consideration of other π_y mixing does not improve insight into central site preference. The C–C overlap population in the Mulliken sense decreases from 0.93 in the centered site to 0.90 in the bridging site, consistent with the fact the barrier to dissociation is less at the latter.

Acetylene chemisorbs to Ni_4S_4, see Fig. 2, but since $\Delta I = 1$ for Ni and though the S 3*p* levels lie just over 2 eV beneath the Fermi level, there is no special advantage to C–C bond scission. In fact, in the central site the barrier increases. The bridged site is not allowed, but if it were the wedging effect would probably be operative, as for O.

Selenium at quarter-monolayer coverage inhibits acetylene chemisorption. On Ni_4Se_4 when the C–C bond stretches 0.2 Å and the HCC angle is 120° and the height is 1.55 Å, a 2 kcal/mole repulsion is calculated. Thus on a larger model weak chemisorption may occur. With Te the interaction should be more repulsive.

The wedge effect should occur on other metal surfaces. Fe is considered in a later section.

VIII. CHALCOGEN BONDING TO Fe(100): SPIN UNPAIRING

The structure and energy levels for oxygen on Fe(100) have already been treated

with the ASED theory (*31*), showing corroboration for dynamic LEED (*32*) and photoemission (*33*) studies. In Ref. (*31*), ΔI is 1.5 eV for Fe and -2.0 eV for O. Energy levels are occupied up to the top of the Fe *d* band, necessitating high-spin orbital occupations.

Since S and Se on Fe(100) have not been examined theoretically before, it is necessary to do so here before considering acetylene chemisorption on chalcogenated Fe(100). First, FeS and FeSe molecules are considered. For them ΔI is taken as 1 eV for Fe. The orbital exponents for Fe are, as the ionization energies, from Ref. (*31*). These and other parameters are in Table 1. Ionization energies for S and Se are the same as for the above Ni study, but orbital exponents are decreased by 0.1 in response to charge transfer. S and Se should be more negative than -0.1 and 0.1, the respective Mulliken charges on Ni_4, because Fe is less electronegative, its 3*d* band lying 1 eV higher. Calculated charges are -0.78 for S and -0.20 for Se.

Calculated FeS and FeSe spectroscopic properties are in Table 3. Diatomic states assumed to be $^7\Sigma$ with the corresponding configuration, $1\sigma^2\,2\sigma^2\,1\pi^4\,1\delta^2\,3\sigma^1\,2\pi^2\,4\sigma^1$, where the δ orbitals have chalcogen character. Since the chalcogen orbital exponents are more diffuse than for Ni chalcogenides, E_R is greater, contributing to the 0.16-Å-greater calculated bond lengths. With this larger equilibrium distance, and since $Z_{Fe} \simeq$

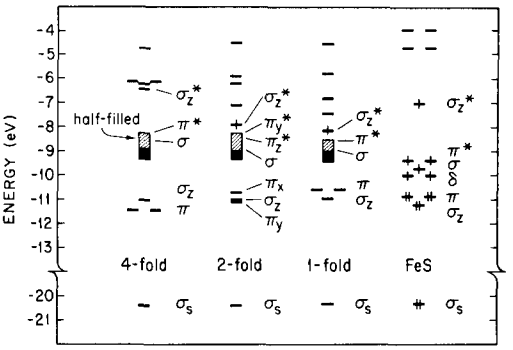

FIG. 11. Energy levels for FeS and Fe_4S with S in four-, two- and onefold sites at equilibrium.

Z_{Ni}, the force constant, via the Poisson equation (*18*), is only slightly over half as much as for the diatomic Ni species. It would help to have experimental values for these bond lengths to optimize the chalcogen orbital exponents.

When electrons are unpaired up to the gaps in Figs. 11 and 12, Fe_4S and Fe_4Se show fourfold centered binding sites to be preferred on the Fe(100) surface. These energy levels are for the calculated equilibrium distances in Figs. 13 and 14. Note how energy levels identified for FeS and FeSe also are found in the surface species in Figs. 11 and 12. Similarities between FeS and FeSe and onefold site binding curves are found in Figs. 13 and 14. These similarities are chemically reasonable. For the Fe_4 surface model ΔI is 0 for Fe so that S and Se charges are -0.47 and -0.004 electron, respectively, in the fourfold sites. A dy-

TABLE 3

Calculated and Experimental Bond Lengths, R_e, Stretching Force Constants, k_e, Ionization Potentials, IP, and Dissociation Energies for $^7\Sigma$ FeS and FeSe

Molecule	R_e (Å)	k_e (mdyn/Å)	IP (eV)	D_e (kcal/mole)
FeS	2.19	1.44	7.07	55(76.3 ± 3)[a]
FeSe	2.29	1.42	7.05	45

[a] B. Rosen (Ed.), "Spectroscopic Data Relative to Diatomic Molecules." Elmsford, N.J., Pergamon, 1970.

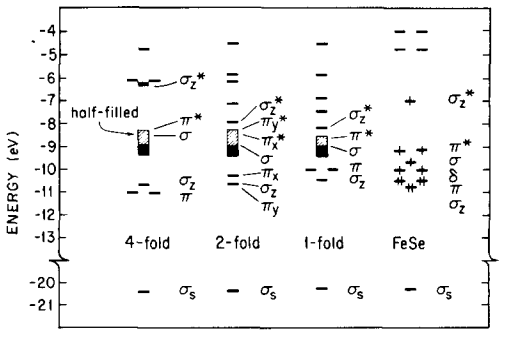

FIG. 12. As in Fig. 11, but for Se.

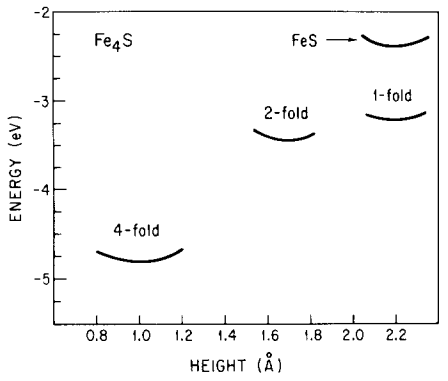

FIG. 13. Binding energy curves for FeS and Fe_4S with S in four-, two- and onefold sites. As discussed in the text, spin pairing will raise the fourfold site curve about 1 eV.

namic LEED study of S on Fe(100) (*34*) favors the fourfold site at 1.09 ± 0.05 Å from the surface, close to the calculated 1.0 Å. On two- and onefold sites calculated chalcogen charges are much larger. Small work function changes for S and Se on Fe(100) would corroborate the finding of fourfold coordination.

Although the σ_z^* level is taken to be occupied by one electron in FeS and FeSe and one- and twofold Fe_4S and Fe_4Se, in the fourfold sites it is empty. There are 12 unpaired electrons for the one- and twofold sites and 10 for the fourfold sites. Since electrons unpair in order to reduce coulombic repulsions, the driving force to occupy the σ_z^* orbital should be decreased on the surface where adsorbate-surface orbital electrons can delocalize to an extent. If this were not the case, then these calculations would predict preference for the twofold sites. Chalcogen chemisorption serves to decrease the number of unpaired electrons in the Fe_4 model from 12 to 10. The net result of this spin pairing is an increase in electron repulsion. The energy difference between the spin 12 and spin 10 clusters is approximately (*35*)

$$E_{12} - E_{10} \simeq J_{12} - \tfrac{1}{2}(J_{11} + J_{12}) + \frac{(e_1 - e_2)^2}{2K_{12}}, \quad (4)$$

where J and K are coulomb and exchange integrals for the δ and σ_z^* orbitals and e_1 and e_2 are corresponding orbital energies. A reduction in the magnitude of the J_{11} and J_{22} coulomb integrals favors low spin, and electron delocalization leads to this. The additional electron repulsion energy relative to the two- and onefold sites will weaken the bonding to the fourfold sites from that shown in Figs. 13 and 14. This weakening should be about 1 eV, approximately the δ–σ_z^* splitting for the two- and onefold sites. Decreasing fourfold site binding energies 1 eV causes the three minima in Figs. 13 and 14 to lie on lines. This reduces calculated chemisorption energies for Fe_4S and Fe_4Se to 87 and 83 kcal/mole, respectively. These electron pairing phenomena will no doubt be recurrent and may play an important role in understanding chemisorption in some instances.

While these Fe_4S and Fe_4Se cluster results are used in the acetylene chemisorption study to follow, a few additional comments on the model are made first. As expected, when the S and Se orbital exponents are not decreased by 0.1, distances to the surface shorten. They become 0.82 Å for S and 0.94 Å for Se, using both Fe_4 and Fe_5 clusters. The Fe_5 cluster has an atom from the next monolayer centered beneath the square. However, when the 0.1 decrease is retained, the heights above the Fe_4

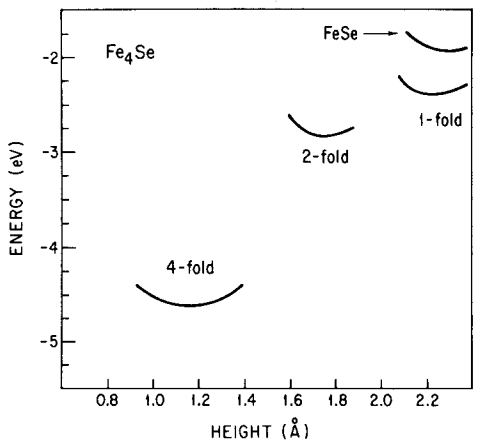

FIG. 14. As in Fig. 13, but for Se.

clusters increase about 0.2 Å. On an Fe_9 cluster, with five additional atoms in the second layer, when S is 1.1 Å above the surface the π^* levels lie at 7.53 eV and the σ_z^* level at 7.58 eV. The π levels are pushed up about 1 eV and the σ_z^* level down the same amount. The binding energy curve shows a softening, being nearly flat from 0.9 to 1.3 eV, provided the S exponents are not decreased by 0.1. The binding energy is reduced to about 65 kcal/mole. While the larger exponents prefer a larger distance on Fe_4 akin to the dynamic LEED value of 1.09 ± 0.05 Å, it is possible that on Fe_4 the shorter distance 0.82 Å is more accurate. This is an unusually strong model size effect, compared with past studies in Refs. (*21*) and (*31*).

IX. CHEMISORPTION AND DISSOCIATION OF ACETYLENE ON O-, S- AND Se-COVERED Fe(100) SURFACES

The chemisorption interaction between acetylene and iron is much greater than that with nickel, predominantly because the Fe 3*d* orbitals are more diffuse, an effect shown in (*5*). The approximate d^9 character of bulk Ni compared to the approximate d^7 character of bulk Fe means for Ni compounds more antibonding molecular orbitals are occupied, aiding in reducing chemisorption energies.

On Fe_5 acetylene strongly chemisorbs as shown in Fig. 15. Spontaneous dissociation yields CH fragments, as found in (*3*, *4*). Binding to this surface is twice as strong as for Ni(100). A model "chemisorbed acetylene" geometry with 0.2-Å increase in the C–C bond length, an HCC angle of 125°, and a height of 1.3 Å is used. The CH fragments are calculated to lie 1.2 Å above the surface in bridging positions. On the centered sites on Fe_5O_4, Fe_5S_4, and Fe_5Se_4 clusters the activation energy to C–C bond scission is small. Because of the chemisorption model, on Fe_5O_2, Fe_5S_2, and Fe_5Se_2, scission in bridging sites has a negative barrier of just over 1 eV. In these calculations the clusters with four chalcogen

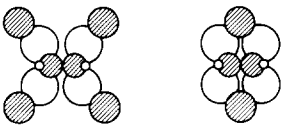

	BE	EA	BE	EA
	(kcal/mole)			
–	79	-16	79	-16
O	36	9	50	-26
S	59	2	58	-25
Se	55	-2	50	-24

FIG. 15. As in Fig. 2, but for Fe. The model chemisorbed acetylene geometry has a 0.2-Å C–C bond stretch, a 120° HCC angle, and a height of 1.3 Å from the surface. The CH fragments are calculated to sit 1.2 Å from the surface, C end down.

atoms have 20 unpaired electrons and those with two such atoms have 14 unpaired electrons. The increase in I for Fe is 1.5 eV. For C and H, $\Delta I = -1$ eV. When acetylene chemisorbs on the sulfide and selenide surfaces, $\Delta I = 1$ eV for Fe, as when acetylene chemisorbs on the pure surface. That is, the acetylene is taken to dominate ΔI for Fe when S and Se do not change it. Further such adjustments will not provide further insight.

Overall, the decrease in two-body repulsion, E_R, for dissociative chemisorption in these calculations is 1.5 kcal/mole. As for Ni(100), there is wedging effect by the chalcogen atoms, aiding C–C bond scission. The total π_y stabilization on Fe_5O_2 compared with Fe_5 is 20 kcal/mole.

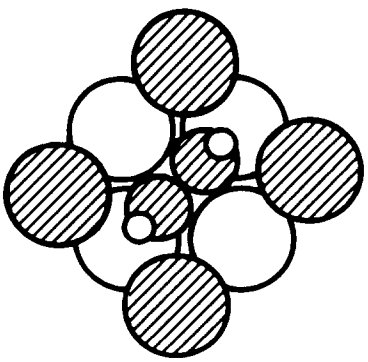

FIG. 16. Acetylene weakly chemisorbed on Fe_4O_4 model of the $c(2 \times 2)$ oxygen-covered (100) surface.

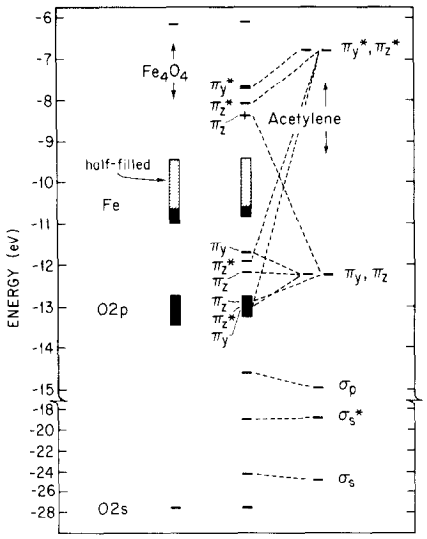

FIG. 17. Energy levels of acetylene, Fe_4O_4 and the chemisorption complex in Fig. 16. As argued in the text, the high-lying half-filled acetylene π_z-surface antibonding orbital should be empty.

While acetylene is repelled by the (2 × 2) half-monolayer S- and Se-covered model in Fig. 16, on Fe_4O_4 the repulsion is only 11 kcal/mole with a C–C bond stretch of 0.2 Å, an HCC angle of 120°, and a height of 1.6 Å. The decrease in E_R is large, 40 kcal/mole. Figure 17 shows the energy levels of acetylene in this geometry. There are 16 unpaired electrons. The acetylene π_y and π_z orbitals form bonding and antibonding combinations with O 2*p* character, and, of course, Fe bonding character. To assist in the unpairing of 16 electrons the high-lying π_z–Fe antibonding orbital must be filled. As argued in Section VIII, this electron is likely to drop back into the Fe *d* band with a gain of ~1 eV. This would result in a weak but attractive chemisorption energy of 12 kcal/mole. Examples of spin pairing with hydrogen chemisorption have been noted (*36*), giving precedent to the pairing hypothesis.

X. CONCLUDING COMMENTS

The ASED theory has been used to make predictions of acetylene structures and bond scission reaction properties on pure and modified Fe(100) and Ni(100) surfaces. Although chalcogen atoms at quarter monolayer and greater coverages on these surfaces weaken or passivate these surfaces toward acetylene chemisorption, in certain circumstances, oxygen is found to activate the Ni(100) surface to carbon bond scission. This occurs as a result of chemisorbed oxygen atoms forcing Ni atoms into hybridizations favoring weakened associative chemisorption and thereby putting the adsorbed acetylene closer in energy to the transition state. Other predictions include the weakening of the carbon bond scission energy when a Ni(100) surface is charged positive or negative as an electrode in a dielectric medium. This is a complicated result of shifting the metal valence band and changing the metal atom ionization energies. This procedure shows promise for modeling electrodes in the future.

Questions of electron spin pairing and its structural effects in the systems studied are brought up. The understanding of the effects of spin pairing and unpairing on structures and activity is seen to be a worthwhile area for further theoretical development. From the experimental viewpoint, the spin unpairing rule used here has been postulated by others, with electrons unpairing over levels spanning up to 1.5 eV in order to occupy levels in the *d* band (*37*). How external fields or structural perturbations relate to this rule is also an interesting experimental question.

REFERENCES

1. Donath, E. E., *Advan. Catal.* **8**, 239 (1956).
2. These and other catalytic reactions are discussed in numerous reviews, including Basolo, F., and Burwell, R. L. (Eds.) "Catalysis Progress in Research," Plenum, New York, 1973; Emmett, P. H., Sabatier, P., and Reid, E. E., "Catalysis Then and Now," Franklin, Inglewood, N.J., 1965; Bond, G. C., "Catalysis by Metals," Academic Press, London/New York, 1962; Anderson, J. R. (Ed.), "Chemisorption and Reactions on Metallic Films," Academic Press, New York, 1971.
3. Anderson, A. B., *J. Amer. Chem. Soc.* **99**, 696 (1977).
4. *a*. Brucker, C. F., and Rhodin, T. N., *J. Catal.* **47**, 214 (1977).

b. Rhodin, T. N., Brucker, C. F., and Anderson, A. B., *J. Phys. Chem.* **82**, 894 (1978).
5. Anderson, A. B., *J. Amer. Chem. Soc.* **100**, 1153 (1978).
6. Demuth, J. E., and Eastman, D. E., *Phys. Rev. Lett.* **33**, 1123 (1974).
7. Demuth, J. E., *Surface Sci.* **80**, 367 (1979).
8. Kesmodel, L. L., Dubois, L. H., and Somorjai, G. A., *Chem. Phys. Lett.* **56**, 267 (1978).
9. Ibach, H., and Lehwald, S., *J. Vac. Sci. Technol.* **15**, 407 (1978).
10. Anderson, A. B., and Hubbard, A. T., *Surface Sci.* **99**, 384 (1980).
11. *a.* Demuth, J. E., and Ibach, H., *Surface Sci.* **85**, 365 (1979).
b. Demuth, J. E., *Surface Sci.* **84**, 315 (1979).
12. Yu, K. Y., Spicer, W. E., Lindau, I., Pianetta, P., and Lin, S. F., *J. Vac. Sci. Technol.* **13**, 277 (1976).
13. Demuth, J. E., and Eastman, D. E., *Phys. Rev. B* **13**, 1523 (1976).
14. This effect and the possibility of nonlinear relaxation shifts are discussed in the literature. See Ley, L., Kowakzyk, S. P., McFeeley, R. T., Pollak, R. A., and Shirley, D. A., *Phys. Rev. B* **8**, 2392 (1973).
15. Mulliken, R. S., *Rev. Mod. Phys.* **14**, 204 (1942); *J. Amer. Chem. Soc.* **77**, 887 (1955); Walsh, A. D., *J. Chem. Soc.* 2260, 2266, 2288, 2296, 2301 (1953); *Progr. Sterochem.* **1** (1954).
16. Anderson, A. B., *Chem. Phys. Lett.* **35**, 498 (1975).
17. Dirac, P. A. M., "Principles of Quantum Mechanics," Sect. 52. Oxford Univ. Press, London, 1930. The details of this time-dependent perturbation procedure will be published separately. See Ref. (*5*) for another viewpoint on the procedure used in this paper.
18. Anderson, A. B., *J. Chem. Phys.* **62**, 1187 (1975).
19. Demuth, J. E., *Phys. Rev. Lett.* **40**, 409 (1978).
20. Whangbo, M. H., and Hoffmann, R., *J. Chem. Phys.* **68**, 5498 (1978).
21. Anderson, A. B., *J. Chem. Phys.* **66**, 2173 (1977).
22. Shigehara, Y., and Ozaki, A., *J. Catal.* **31**, 309 (1973).
23. Anderson, A. B., *J. Vac. Sci. Technol.* **15**, 616 (1978).
24. Demuth, J. E., Jepsen, D. W., and Marcus, P. M., *Phys. Rev. Lett.* **31**, 540 (1973); Van Hove, M., and Tong, S. Y., *J. Vac. Sci. Technol.* **12**, 230 (1975).
25. Walch, S. P., and Goddard, W. A., III, *Solid State Commun.* **23**, 907 (1977); *Surface Sci.* **72**, 645 (1978).
26. Conrad, H., Ertl, G., Kuppers, J., and Latta, E. E., *Solid State Commun.* **17**, 497 (1975).
27. Hagstrum, H. D., and Becker, G. E., *Proc. Roy. Soc. (London) A* **331**, 395 (1972).
28. Hagstrum, H. D., *J. Vac. Sci. Technol.* **12**, 7 (1975).
29. Demuth, J. E., private communication.
30. Hoffmann, R., *Accounts Chem. Res.* **4**, 1 (1971).
31. Anderson, A. B., *Phys. Rev. B* **16**, 900 (1977).
32. Legg, K. O., Jona, F. P., Jepsen, D. W., and Marcus, P. M., *J. Phys. C* **8**, 2492 (1975).
33. Brucker, C. F., and Rhodin, T. N., *Surface Sci.* **57**, 523 (1976).
34. Legg, K. O., Jona, F., Jepsen, D. W., and Marcus, P. M., *Surface Sci.* **66**, 25 (1977).
35. Hay, P. J., Thibeault, J. C., and Hoffmann, R., *J. Amer. Chem. Soc.* **97**, 4884 (1975).
36. Selwood, P. W., "Chemisorption and Magnetization," Academic Press, New York, 1975.
37. Stearns, M. B., and Shinazaki, S. S., *Physica B* **86–88**, 1195 (1977).